Progress In Electromagnetics Research Letters, Vol. 29, 51–64, 2012

APPLICATION OF THE COSINE WINDOW FUNCTION WITH THE PARAMETERS OPTIMIZED BY GENETIC ALGORITHM IN BISTATIC PLANAR NEAR-FIELD SCATTERING MEASUREMENTS

D. Yu, W. Zhai*, G. Xie, and D. Fu

National Key Laboratory of Antennas and Microwave Technology, Xidian University, Xi'an, Shaanxi 710071, China

Abstract—The cosine window function with the parameters optimized by Genetic Algorithm (GA) is applied in bistatic planar near-field scattering measurements so as to effectively improve the measurement precision. With the infinitely long ideal conductor cylinder as the target under test, the bistatic planar near-field scattering measurement technique is studied by the method of computer simulation and some useful results and basic laws are obtained. The calculation results show that the truncation errors caused by finite scan plane in the far-field Radar Cross Section (RCS) of the target under test obtained by near-field to far-field transformation can be reduced greatly by the weighting process of the measured scattered near-field data by means of the cosine window function with the parameters optimized by GA.

1. INTRODUCTION

Near field measurement technique does not need very large measurement range outdoor and has a series of advantages such as large information quantity obtained, high measurement precision, little interference from outside, good keeping secret property etc., therefore as the rapid development of near-field antenna measurement technique [1, 2], near-field measurement technique is also studied to determine the scattering characteristics of targets [3]. By means of planar near-field scattering measurement technique, not only the

Received 15 October 2011, Accepted 9 December 2012, Scheduled 19 January 2012

* Corresponding author: Weigang Zhai (xidian_2010@qq.com).

monostatic scattering characteristics of the target but also the far field RCS in the angle range near the normal direction outside the scan plane can be measured in the case that the target is not rotated, thus the far field scattering characteristics of the target in the case that the bistatic angles are different can be obtained [4].

In general, the scattered field of the target is distributed in a wide range, thus it is usually required that the width of the scan plane should be large enough so as to reduce the truncation errors caused by finite scan plane. However in practical bistatic planar near-field scattering measurements, the width of scan plane is always limited and the truncation level is not always very low, sometimes even relatively high. In this case, the truncation errors caused by finite scan plane are generally large. In order to reduce the truncation errors and improve the measurement precision, the cosine window function is introduced and applied in the bistatic planar near-field scattering measurements [5]. The appropriate choice of the parameters of the cosine window function has significance for improving the measurement precision. In this paper, the cosine window function with the parameters optimized by Genetic Algorithm (GA) is applied in the bistatic planar near-field scattering measurements so as to greatly reduce the truncation errors caused by finite scan plane.

2. COSINE WINDOW FUNCTION

From the theory of near-field to far-field transformation in bistatic planar near-field scattering measurements, the far-field scattering characteristics of the target can be evaluated from the scattered near field by Fourier transform. With the two-dimensional problem as an example, it is assumed that the scattered near field is $f(x)$ and the Fourier transform of which is $F(k)$. In practical bistatic planar near-field scattering measurements, only the scattering near fields in the finite scan plane are assumed to be zero. Therefore, the scattered near field $f_w(x)$ utilized to evaluate the far-field scattering characteristics of the target can be express as the following equation.

$$f_w(x) = f(x) \cdot w(x)$$

where $w(x)$ is the rectangle window function. If the width of the scan plane is assumed to be W, $w(x)$ can be expressed as

$$w(x) = \begin{cases} 1, & |x| \leq w/2 \\ 0, & |x| > w/2 \end{cases}$$

It is assumed that the Fourier transforms of $f_w(x)$ and $w(x)$ are

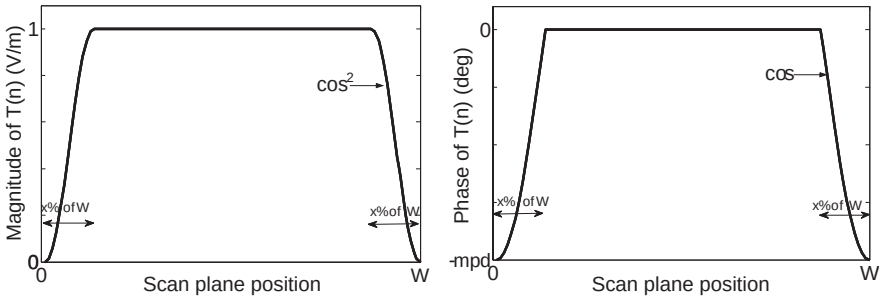

Figure 1. The magnitude and phase distribution of the cosine window function, (a) magnitude distribution, (b) phase distribution.

$F_w(k)$ and $\tilde{w}(k)$ respectively. Then from the theory of signal process, $F_w(k)$ is equivalent to the convolution of the two corresponding Fourier transforms $F(k)$ and $\tilde{w}(k)$ [6], i.e.,

$$F_w(k) = F(k) * \tilde{w}(k)$$

where the symbol "$*$" denotes the convolution.

In order to accurately evaluate the far-field scattering characteristics of the target from the measured near field, we should try to make $F_w(k)$ approach to $F(k)$, which requires that the main-lobe of the Fourier transform $\tilde{w}(k)$ should be narrow enough and the peak value of the side-lobe small enough. The Fourier transform of the rectangle window function has narrow main-lobe, but also large peak value of the side-lobe. Therefore, the rectangle window function may not be the optimum window function. In this paper, we try to find a better window function to substitute the rectangle window function and weight the scattered near field data so as to improve the precision of bistatic planar near-field scattering measurements.

The window function is also called weighting function. It is assumed that the number of sampling points is N and the sampling interval ds, then the width of the scan plane is $W = (N-1) \cdot ds$. Figure 1 shows the magnitude and phase distribution of the cosine window function.

If the cosine window function is assumed to be the following equation:

$$T(n) = A(n)e^{jP(n)} \quad n = 1, 2, 3, \ldots, N$$

Then $A(n)$ and $P(n)$ can be expressed as the following equations

respectively:

$$A(n)=\begin{cases}\dfrac{1}{2}\left\{1-\cos\left[\dfrac{(n-1)\cdot ds\cdot\pi}{W\cdot x\%}\right]\right\} & 1\le n\le 1+(N-1)\cdot x\% \\ 1 & 1+(N-1)\cdot x\%<n \\ & \le 1+(N-1)(1-x\%) \\ \dfrac{1}{2}\left\{1-\cos\left[\dfrac{(n-1)\cdot ds\cdot\pi-W\cdot\pi}{W\cdot x\%}\right]\right\} & 1+(N-1)(1-x\%)<n\le N\end{cases}$$

$$P(n)=\begin{cases}-mpd\cdot\cos\left[\dfrac{(n-1)\cdot ds\cdot\pi}{2W\cdot x\%}\right] & 1\le n\le 1+(N-1)\cdot x\% \\ 0 & 1+(N-1)\cdot x\%<n \\ & \le 1+(N-1)(1-x\%) \\ -mpd\cdot\cos\left[\dfrac{(n-1)\cdot ds\cdot\pi-W\cdot\pi}{2W\cdot x\%}\right] & 1+(N-1)(1-x\%)<n\le N\end{cases}$$

where $x\%$ is the proportion of the distance between the tapering point and the edge to the whole width of the scan plane; mpd is the maximum phase delay of the edge relative to the tapering point and $n=1,2,3,\ldots,N$.

Compared with the Fourier transform of the rectangle window function, the Fourier transform of the cosine window function has a little wider main-lobe, but much smaller peak value of the side-lobe. As mentioned in Section 1, in practical bistatic planar near-field scattering measurements, because the scattered field of the target is distributed in a wide range and the width of the scan plane is always limited, the truncation level at the side of the scan plane is not always very low, sometimes even relatively high. In this case, if the traditional rectangle window function is utilized to weight the measured scattered near field data, because the scattered near fields outside the scan plane are assumed to be zero, the discontinuity of the scattered near fields at the side of the scan plane is very obvious, which will introduce large truncation errors in the measurement results. However, if the cosine window function is utilized to weight the measured scattered near field data, because the scattered near fields at the side of the scan plane are set to be zero, the discontinuity of the scattered near fields at the side of the scan plane can be overcome, which will greatly reduce the truncation errors in the measurement results. Therefore in bistatic planar near-field scattering measurements, the cosine window function is better than the traditional rectangle windows function for improving the measurement precision. There are two important parameters ($x\%$ and mpd) in the cosine window function. The measurement precision can be effectively improved by appropriate choice of the two parameters. In this paper, Genetic Algorithm (GA) is utilized to

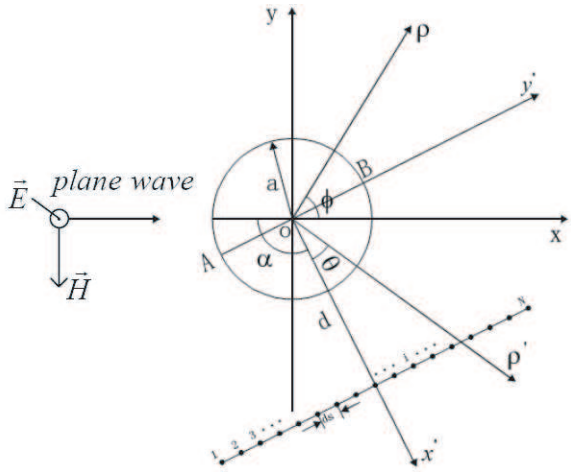

Figure 2. Illustration of the calculation model.

optimize the two parameters so as to greatly improve the measurement precision.

3. CALCULATION MODEL

As shown in Figure 2, the incident ideal plane wave with the expression of $\vec{E}^i = \hat{z}E_0e^{-jkx}$ (k is the wave number) is transmitted vertically toward the infinitely long ideal conductor cylinder, the radius of which is a. It is assumed that d is the distance between the scan plane and the center of the cylinder and that α ($-\pi \leq \alpha \leq \pi$) is the angle formed by the direction inverse to the incident plane wave from the center of the cylinder (i.e., the direction of $-x$) and the direction of the straight line vertical to the scan plane from the center of the cylinder (i.e., the direction of x'). The number of sampling points is N and the sampling interval ds, so the width of the scan plane is $W = (N-1) \cdot ds$.

From the electromagnetic field theory [7], the theoretical far-field RCS of the infinitely long ideal conductor cylinder is expressed as the following equation

$$\sigma(\phi) = \lim_{\rho\to\infty} 2\pi\rho\frac{|E_z^s|^2}{|E_y^i|^2} = \frac{4}{k}\left|\sum_{n=-\infty}^{\infty}\frac{J_n(ka)}{H_n^{(2)}(ka)}e^{jn\phi}\right|^2 \approx \frac{4}{k}\left|\sum_{n=-N}^{N}\frac{J_n(ka)}{H_n^{(2)}(ka)}e^{jn\phi}\right|^2$$

$$= \frac{2\lambda}{\pi}\left|\frac{J_0(ka)}{H_0^{(2)}(ka)} + 2\sum_{n=1}^{N}\frac{J_n(ka)}{H_n^{(2)}(ka)}\cos(n\phi)\right|^2$$

where λ is wavelength; the value of N can be taken as $N = INT(ka + 9)$; the symbol "INT" denotes taking integer; J_n is the first kind of Bessel function with n order; $H_n^{(2)}$ is the second kind of Hankel function with n order.

The process of computer simulation is as follows:

Firstly, the scattered near fields $E_z^s(i)$ $(i = 1, 2, 3, \ldots, N)$ produced at the sampling points as the ideal plane wave is transmitted vertically toward the infinitely long ideal conductor cylinder are calculated. Then the scattered near-field data are dealt with by means of the cosine window function introduced above and the scattered fields outside the scan plane are assumed to be zero, and so the weighted scattered near fields $E_z^s(m)$ $(m = 0, 1, 2, \ldots, N'' - 1)$ are obtained. Finally, from the theory of near-field to far-field transformation, the far-field RCS can be evaluated by the following formula, which can be effectively calculated by means of fast Fourier transform (FFT) [4, 8].

$$\sigma(\theta) = \frac{k}{|E_0|^2} \cos^2\theta ds^2 \left| \sum_{m=0}^{N''-1} E_z^s(m) e^{j\frac{2\pi mn}{N''}} \right|^2$$

where the value of N'' can be taken as $N'' = 2048 = 2^{11}$ and the relationship between n and θ is given by

$$n = \frac{N'' \cdot ds}{\lambda} \sin\theta, \quad n = -\frac{N''}{2}, -\frac{N''}{2} + 1, \ldots, \frac{N''}{2} - 1$$

In this paper, GA is utilized to optimize the selection of the parameters ($x\%$ and mpd) for the cosine window function in bistatic planar near-field scattering measurements. GA is mainly composed of three operators: reproduction, crossover and mutation [9–16]. It is operated in the following steps:

1) create an initial population;
2) evaluate the fitness of each population member;
3) invoke natural selection;
4) select population members for mating;
5) generate offspring;
6) mutate selected members of the population;
7) terminate run or go to step 2).

Here we use roulette wheel method as the selection operator and single point crossover operator as the crossover operator. Crossover rate is 0.6, and we take basic bit mutation operator as the mutation operator. Mutation rate is 0.001, and binary coding is taken as the individual encoding. Population size is up to 100 and operation steps

size 400. Optimization precision is 0.001 for $x\%$ and 1° for mpd. Individual fitness function is:

$$fitness = \sum_i |RCS\_theory(i) - RCS\_test(i)|$$

where RCS_theory and RCS_test are the dB values of the far-field RCS calculated theoretically and the far-field RCS evaluated by near-field to far-field transformation, respectively. The search range for $x\%$ is from 0 to 0.5, and that for mpd is from 0° to 360°.

4. CALCULATION RESULTS AND DISCUSSION

By means of the calculation model established above, bistatic planar near-field scattering measurements are studied by the method of computer simulation with the infinitely long ideal conductor cylinder as the target under test and some useful results are obtained.

In order to study the effect of near-field data processing method on the measurement results, in the case that other conditions are not changed, the scattered near-field data are dealt with by means of the cosine window functions with different window parameters ($x\%$ and mpd) respectively and without using the cosine window function (i.e., the window parameters are taken as $x = 0\%$, $mpd = 0°$), then the RCS curves in the angle range $[-30°, 30°]$ relative to the x' axis are calculated by means of near-field to far-field transformation respectively and compared with the theoretical RCS curve.

In the following calculation, the parameters are taken as $f = 9375\,\text{MHz}$, $a = 2\lambda$, $\alpha = 120°$, $d = 6\lambda$, $N = 47$, $ds = 0.5\lambda$. Here we choose two sets of different window parameters: the first one is $x\% = 30\%$, $mpd = 90°$; the second one is $x\% = 40\%$, $mpd = 120°$. The calculation results are shown in Figure 3.

It can be seen that the deviation between the RCS curve obtained by using the cosine window function and the theoretical RCS curve is much smaller than the deviation between the RCS curve obtained without using the cosine window function and the theoretical RCS curve, which proves the validity of dealing with the scattered near field data by means of cosine window function. Furthermore, the deviation between the RCS curve obtained as the first set of window parameters are taken, and the theoretical RCS curve is smaller than the deviation between the RCS curve obtained as the second set of window parameters are taken and the theoretical RCS curve. Therefore, the results obtained by selecting different window parameters are different, and the selection of appropriate window parameters has significance for improving the measurement precision.

By selecting different window parameters and comparing the corresponding RCS curves obtained with the theoretical RCS curve, we find out a better set of window parameters, i.e., $x\% = 13\%$, $mpd = 20°$ (the third one). The calculation results are shown in Figure 4.

It can be seen that the RCS curve obtained as the third set of window parameters is more close to the theoretical RCS curve than the RCS curves obtained before with the first and second sets of window

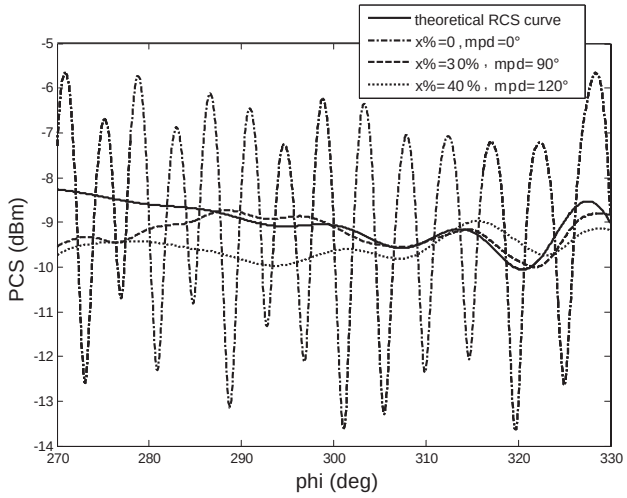

Figure 3. The comparison of RCS curves obtained in different cases.

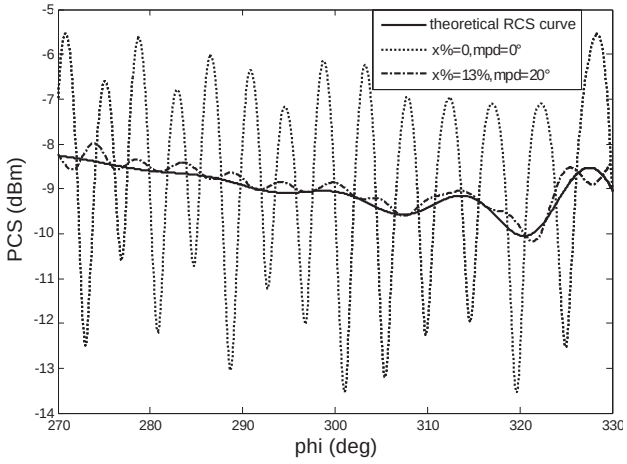

Figure 4. The comparison of RCS curves.

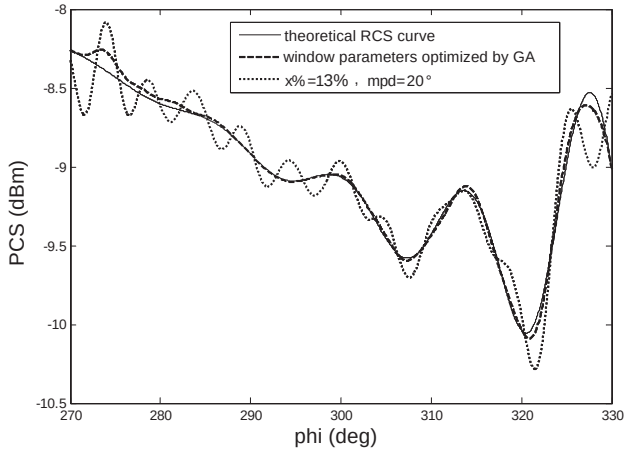

Figure 5. The comparison of RCS curves.

parameters are selected, respectively. But the selected parameters of cosine window function may not be the optimal parameters. Here Genetic Algorithm (GA) as described in Section 3 is utilized to determine the optimal parameters of cosine window function so as to improve the measurement precision at most. The optimal parameters obtained are $x\% = 25\%$, $mpd = 15.499^\circ$ and the corresponding calculation results are shown in Figure 5.

It can be seen that the RCS curve obtained with the parameters of cosine window function optimized by GA agrees with the theoretical RCS curve is much better than the RCS curve obtained as the third set of window parameters (i.e., $x\% = 13\%$, $mpd = 20^\circ$) are taken.

If the value of the angle α is changed, the parameters of cosine window function can also be optimized by GA, and the corresponding RCS curve can be calculated by near-field to far-field transformation. The calculation results in the cases that $\alpha = 0^\circ$ and $\alpha = -180^\circ$ are shown in Figure 6 and Figure 7, respectively. The corresponding optimal parameters of cosine window function are $x\% = 27.44\%$, $mpd = 12.68^\circ$ and $x\% = 22.7\%$, $mpd = 12.68^\circ$ in the cases that $\alpha = 0^\circ$ and $\alpha = -180^\circ$, respectively.

In the following calculation, the parameters are taken as $f = 9375\,\text{MHz}$, $\alpha = 120^\circ$, $ds = 0.5\lambda$. The window parameters are $x\% = 13\%$, $mpd = 20^\circ$. In the case that the radius of the cylinder and the distance between the scan plane and the center of the cylinder are changed, the RCS in the angle range $[-30^\circ, 30^\circ]$ relative to the x' axis is calculated and compared with the theoretical RCS. Then the minimum number of sampling points needed in order to make

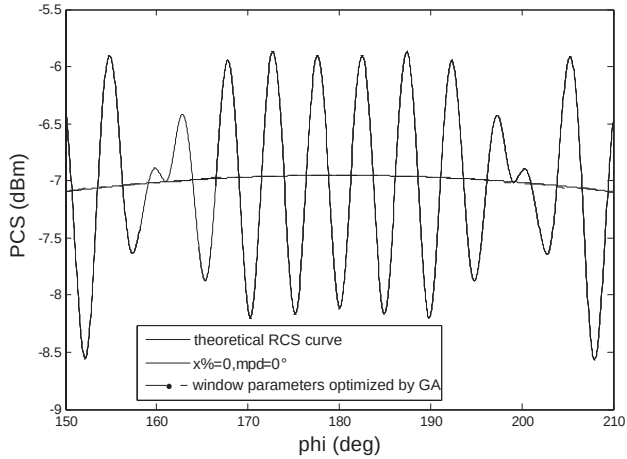

Figure 6. The comparison of RCS curve ($\alpha = 0°$).

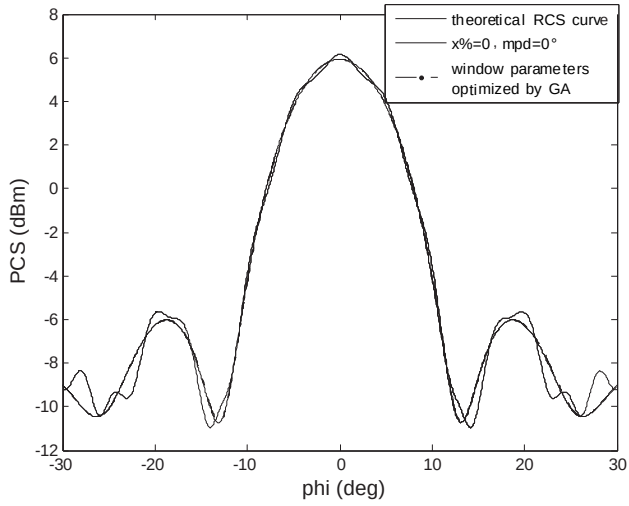

Figure 7. The comparison of RCS curves ($\alpha = -180°$).

the maximum deviation less than 0.5 dB, corresponding width of the scan plane and ratio of the width of scan plane to the diameter of the cylinder are determined. The calculation results are listed in the Table 1 below.

It can be seen from the above results that with the increase of radius of the cylinder, the required minimum width of the scan plane

will also increase, but the ratio $W/2a$ of the minimum width of the scan plane and diameter of the cylinder will reduce. When the radius of the cylinder is increased up to 25λ, the value of $W/2a$ is equal to 2, that is the required minimum width of the scan plane equal to twice of the diameter of the cylinder. Along with a further increase of radius of the cylinder, the value of $W/2a$ gradually decreases. At the same time, it can also be seen that in the case that value a of the radius of the cylinder is remained unchanged, with the increase of value d of the distance between the scan plane and the center of the cylinder, the required minimum width of the scan plane will accordingly increase.

In addition, with the increase of radius of the cylinder, the optimal parameters of the cosine window function will also change. In the case

Table 1. the calculation results in different cases.

$a(\lambda)$	$d(\lambda)$	N	$W(\lambda)$	$W/2a$
2	6	47	23	5.75
5	10	61	30	3.0
10	15	93	46	2.3
10	20	107	53	2.65
15	20	127	63	2.10
20	25	163	81	2.025
20	30	179	89	2.225
25	30	201	100	2.0
30	35	237	118	1.967

Table 2. the optimal parameters of the cosine window function in different cases.

$a(\lambda)$	$d(\lambda)$	N	$x\%$	mpd (degree)
2	6	47	0.25	16
5	10	61	0.16	28
10	15	93	0.14	19
10	20	107	0.13	22
15	20	127	0.13	15
20	25	163	0.12	15
20	30	179	0.11	19
25	30	201	0.08	10
30	35	237	0.07	16

that the radius of the cylinder, the distance between the scan plane and the center of the cylinder and the number of the sampling points are taken the same values as that in Table 1, the corresponding optimal parameters of the cosine window function are obtained by GA. The calculation results are listed in Table 2 below.

It can be seen from Table 2 that with the increase of radius of the cylinder, the optimal value of $x\%$ decreases, i.e., the cosine window function becomes more and more steep near the edge of the scan plane, but the optimal value of *mpd* does not have regular changes.

5. CONCLUSION

In bistatic planar near-field scattering measurements, how to process the measured scattered near-field data so as to reduce the truncation errors caused by finite scan plane and improve the measurement precision is a key problem with very important theoretical and practical significance. In order to solve this problem, the application of the cosine window function with the parameters optimized by Genetic Algorithm (GA) in the bistatic planar near-field scattering measurements is studied by the method of computer simulation with the infinitely long ideal conductor cylinder as the target under test and some useful results and basic laws are obtained. The calculation results show that the truncation errors caused by finite scan plane in the far-field RCS of the target under test obtained by near-field to far-field transformation can be reduced greatly by the weighting process of the measured scattered near-field data by means of the cosine window function with the parameters optimized by GA, which proves the validity and applicability of the near-field data processing method based on the cosine window function with the parameters optimized by GA in the bistatic planar near-field scattering measurements.

ACKNOWLEDGMENT

This work is supported by the National Natural Science Foundation of China (Grant No. 60801038) and the Fundamental Research Funds for the Central Universities (Grant No. K50510020019).

REFERENCES

1. Slater, D., *Near-Field Antenna Measurements,* Artech House, Boston, 1991.
2. Hansen, J. E., *Spherical Near-Field Antenna Measurements,* Peter Peregrinus Ltd, London, 1988.

3. Cown, B. J. and C. E. Ryan, Jr., "Near-field scanning measurements for determining complex target RCS," *IEEE Transactions on Antennas and Propagation*, Vol. 37, No. 5, 576–585, May 1989.
4. Yu, D., "Study of some key problems of planar near-field radiation and scattering measurements," Ph.D. Dissertation, Xidian University, Jan. 2004.
5. Yu, D., D. Fu, Q. Liu, and N. Mao, "Application of the window function in bistatic planar near-field scattering measurements," *IEEE 2007 International Symposium on Microwave, Antenna, Propagation, and EMC Technologies for Wireless Communications*, Nos. 16–17, 891–984, Aug. 2007.
6. Harris, F. J., "On the use of windows for harmonic analysis with the discrete fourier transform," *Proceedings of the IEEE*, Vol. 66, No. 1, 51–83, Jan. 1978.
7. Harrington, R. F., *Time-Harmonic Electromagnetic Fields,* McGraw-Hill Book Company, New York, 1961.
8. Costanzo, S. and G. D. Massa, "Near-field to far-field transformation with planar spiral scanning," *Progress In Electromagnetics Research*, Vol. 73, 49–59, 2007.
9. Haupt, R. L., *Genetic Algorithms in Electromagnetics,* John Wiley & Sons, Inc., Hoboken, New Jersey, 2007.
10. Mahanti, G. K., N. N. Pathak, and P. K. Mahanti, "Synthesis of thinned linear antenna arrays with fixed sidelobe level using real-coded genetic algorithm," *Progress In Electromagnetics Research*, Vol. 75, 319–328, 2007.
11. Su, D. Y., D.-M. Fu, and D. Yu, "Genetic algorithms and method of moments for the design of PIFAs," *Progress In Electromagnetics Research Letters*, Vol. 1, 9–18, 2008.
12. Zhao, Y., F. Chen, H. Chen, N. Li, Q. Shen, and L. Zhang, "The microstructure design optimization of negative index metamaterials using genetic algorithm," *Progress In Electromagnetics Research Letters*, Vol. 22, 95–108, 2011.
13. Siakavara, K., "Novel fractal antenna arrays for satellite networks: Circular ring Sierpinski carpet arrays optimized by genetic algorithms," *Progress In Electromagnetics Research*, Vol. 103, 115–138, 2010.
14. Mahmoudi, A., N. A. Rahim, and H. W. Ping, "Genetic algorithm and finite element analysis for optimum design of slotted torus axial-flux permanent-magnet brushless DC motor," *Progress In Electromagnetics Research B*, Vol. 33, 383–407, 2011.

15. Jain, R. and G. S. Mani, "Dynamic thinning of antenna array using genetic algorithm," *Progress In Electromagnetics Research B*, Vol. 32, 1–20, 2011.
16. Ozturk, N. and E. Celik, "Application of genetic algorithms to core loss coefficient extraction," *Progress In Electromagnetics Research M*, Vol. 19, 133–146, 2011.